Plasma Phys. Control. Fusion **51** (2009) 045001 (9pp) doi:10.1088/0741-3335/51/4/045001

Experimental study of the hard x-ray emissions in a plasma focus of hundreds of Joules

M Barbaglia[1], H Bruzzone[2], H Acuña[2], L Soto[3] and A Clausse[1]

[1] CONICET-CNEA and Universidad Nacional del Centro, 7000 Tandil, Argentina
[2] CONICET and Universidad Nacional de Mar del Plata, 7600, Mar del Plata, Argentina
[3] Comisión Chilena de Energía Nuclear and Center for Research and Applications in Plasma Physics and Pulsed Power, P4, Casilla 188-D, Santiago, Chile

Received 4 November 2008, in final form 8 December 2008
Published 20 January 2009
Online at stacks.iop.org/PPCF/51/045001

Abstract
An experimental study on hard x-ray production in a small plasma focus device operating in a few hundreds of Joule range is presented. A threshold in the voltage drop on the pinch was observed for x-ray emission. A comparison with Dreicer theory for electrons runaway in plasmas yields significant agreement. The study was performed at a constant pressure (1.8 mbar) of deuterium with three different anode lengths.

1. Introduction

Plasma focus (PF) devices are efficient sources of short bursts of hard and soft x-rays, neutrons and ions as well as electron beams. PFs are used in plasma physics research and industrial applications for they have unique qualities such as low cost, compact size, low operation risk (compared with isotopic neutron sources) and offer good performance in terms of the intensity of radiation pulses. Substantial efforts were made to understand the physics of the pulsed emissions, producing scaling laws with different PF devices in the energy range between 0.1 J and 1 MJ [1–3, 16]. Recently, there has been renewed interest in the development of low-energy PF devices of tens or hundreds of Joules, which can be designed as portable devices suitable for a number of applications [4, 5, 16].

Basically a PF is a coaxial gun composed of two cylindrical electrodes placed in a chamber filled with a few millibars of gas. A spark gap connects the anode (inner electrode) with a capacitor bank charged at high voltage. When the spark gap closes, an electrical discharge starts in the gap between the electrodes forming an umbrella-like plasma layer. The Lorentz force pushes the current sheath (CS) toward the open end of the electrodes, collecting the gas particles ahead of it. Finally, the sheath arrives at the anode end, runs over it and collapses radially focusing into a plasma column (called pinch) with ion densities in the range of $\sim 10^{19}$. The lifetime of the pinch is proportional to the anode radius [6]; thus, larger devices of hundred kiloJoules to megaJoules have durations of a few hundred nanoseconds, devices of a few kiloJoules have a duration of tens of nanoseconds and about 10 ns or less in the new generation of fast and compact plasma foci [4, 5, 16].

0741-3335/09/045001+09$30.00

In order to avoid misleading, in what follows 'hard' x-rays mean those which can be detected outside the vacuum chamber, that is, those with energies above 5 keV, while 'soft' mean those which can only be detected inside the chamber, having energies below 5 keV. This 'definition', while purely operational, is important because it distinguishes between two separate sources of radiation. Soft x-rays are generated by thermal bremsstrahlung emission in the hot plasma column and eventually by line radiation of highly stripped ions, if the charging gas has a sufficiently high atomic number (e.g. N, Ne, Ar). In turn, hard x-rays can only be originated by bremsstrahlung of high energy (>5 keV) electron beams extracted from the pinch upon impacting on the anode [7]. These pulses have potential applications in radiography [8], including fast moving objects [15]. In addition, soft x-rays are also produced in the pinch. There is no particular reason for expecting a strong correlation between both forms of emission [9].

In this research, we were mainly interested in the hard x-rays emitted by a low-energy PF device. This component of the radiation has been detected since the very beginning of PF research with time resolution usually using scintillator photomultiplier combinations. Precise measurements of its spectrum have never been done (being a quite difficult measurement due to pile-up effects) but they surely have sizable fractions with energies close to 100 keV (a block of lead several centimeters in width in front of the scintillator reduces the signal roughly by half), and using a set of absorbers having different widths, a 83 keV equivalent peak energy value has been estimated in a recent work [7]. To our knowledge, the dependence of hard x-rays on the design parameters of a PF, especially the geometry of the electrodes, has not been studied.

In this paper, experimental data of the hard x-ray emissions of a small PF device (μSTAR), working between 100 and 300 J, are presented. In particular, different anode lengths were tested studying the influence of the pinch voltage drop on the production of this type of radiation.

2. Experimental setup and procedure

A schematic of μSTAR and its charging circuit is shown in figure 1. The capacitor bank is composed of 8×0.1 μF capacitors connected in parallel, surrounding the spark gap to provide a minimum inductance connection. The bank can be charged with a power supply up to 35 kV. The external inductance L_o (measured with a short circuit on the spark gap) is 65 nH and the inductance added by the connection to the chamber containing the electrodes is 25 nH. The gas filling procedure is to evacuate the discharge chamber with a mechanical pump for several minutes and then fill it with fresh deuterium gas at 1.8 mbar. The pressure is measured by means of a manometer with ± 0.1 mbar accuracy.

Figure 2 shows a diagram of the electrode configuration. The plastic parts are made of polyamide material glued with epoxy. The anode supports are made of bronze and the cathode is a stainless steel back plate. A bronze piece edged at the center hole is attached to the cathode acting as a field intensifier. A Borosilicate tube (10.60 mm OD, 6.30 ID, 10.10 mm length measured from the intensifier tip) is used as an insulator between the electrodes. The plasma gun does not have the usual coaxial cathode, that is, the current sheet is free to move into the radial direction while moving toward the anode end.

A series of discharges varying the charging voltage were performed using different anode lengths (6.20 mm OD). The voltage evolution between electrodes, $V_{\text{anode}}(t)$, was measured with a calibrated fast resistive voltage divider and the time derivative of the discharge current, $\mathrm{d}I/\mathrm{d}t$, with a Rogowski coil. X-rays are detected by a plastic scintillator type EJ-200, located at 1.75 m, from the pinch region. All the signals were recorded using a four-channel digital oscilloscope, 1 GHz BW and 0.8 ns minimum digitalization time.

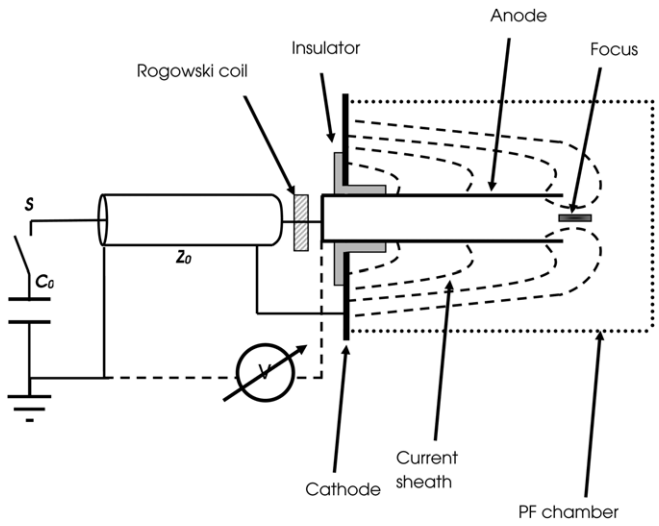

Figure 1. Schematic of a PF device.

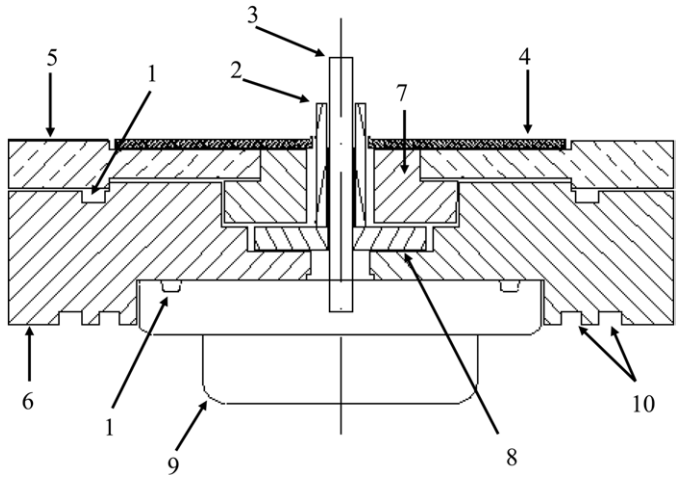

Figure 2. Electrodes configuration. 1: O-ring cavity, 2: insulator, 3: anode, 4: field intensifier, 5: cathode, 6–8: plastic supports, 9: bronze anode back, 10: circular channels to prevent discharges out of the chamber.

3. Results

Three experimental runs were performed using different anode lengths, namely, 30, 28.1 and 23 mm (measured from the insulator open border). The corresponding data are represented by squares, triangles and circles, respectively, in all the figures. All runs were performed at a fixed charging pressure (1.8 mbar), varying the charging voltage between 18 and 28 kV.

Figure 3 shows typical signals of the $V_{\text{anode}}(t)$, $\mathrm{d}I/\mathrm{d}t$ and of the radiation pulse, for a 27 kV shot on the 30.0 mm anode. The pinch is clearly observed in the $\mathrm{d}I/\mathrm{d}t$ signal at $\approx$0.5 μs, with similar spikes on the voltage and on the radiation signals. Since discharges in deuterium can produce fusion neutrons, the pulses registered in the radiation detector must be discriminated

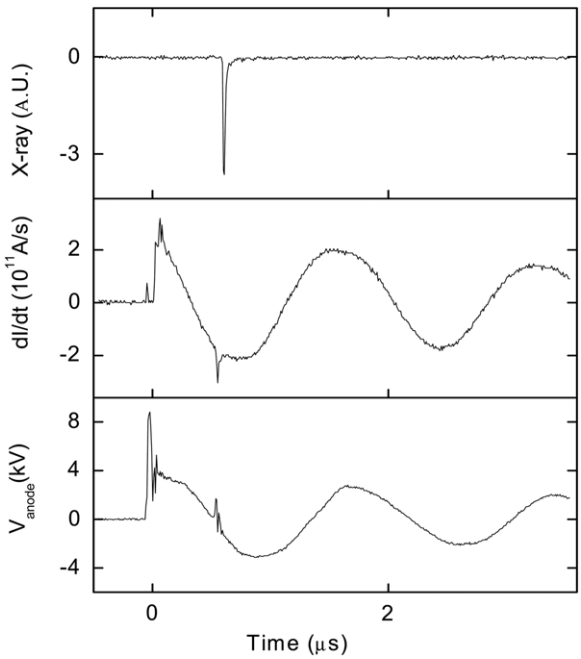

Figure 3. Typical signals of x-ray emission, current derivative and voltage between electrodes (30.0 mm anode length, charging voltage 27 kV).

Table 1. Number of shots performed in each experimental run.

Anode length (mm)	30.0	28.1	23.0
Total number of shots	60	70	60
Pinching shots with radiation production	39	42	36
Pinching shots without radiation production	5	17	13

by the time of flight. However, the distance between the source and the detector required for this discrimination made the neutron pulse very small and in most of the shots below the detection level. It must also be noted that some of the shots only reveal the pinch on the electrical signals, without any corresponding radiation pulse.

Table 1 details the number of discharges measured with and without radiation production. Each signal was processed determining the voltage between electrodes, the current temporal derivative and the radiation peak, at the moment of the pinch. The current at the pinch I_p was calculated by numerical integration. Another relevant magnitude that can be obtained from the signals is the voltage drop along the pinch length, V_p, which can be calculated from the anode voltage and the current derivative, following the procedure proposed in [10]. It should be noted that to calculate V_p the value of the inductance of the gun L'_o is required, which is difficult to know exactly in the present case since the cathode is a base plate. Therefore, L'_o is given by the inductance of the inner connections (25 nH) and the inductance of the CS (excluding the pinch inductance). The latter is much smaller than the former and was then neglected for practical purposes.

Figure 4 shows the dependence of the radiation intensity on V_p, and a clear positive correlation can be recognized, that is, higher V_p produces higher radiation emissions. No

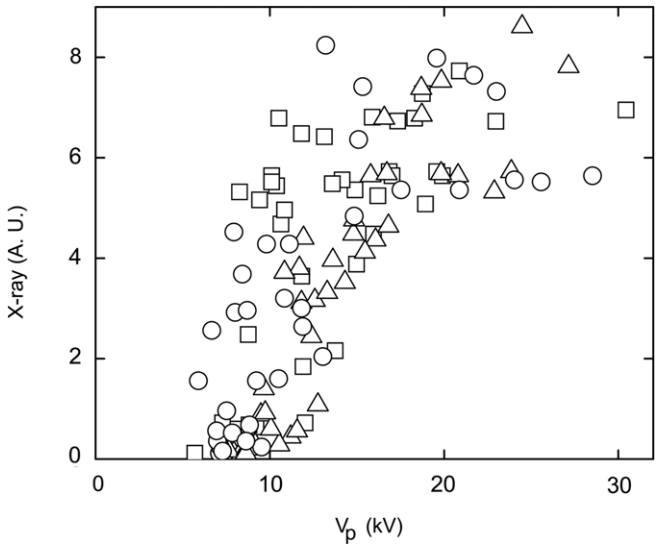

Figure 4. Hard x-ray intensity dependence on the pinch voltage. Anode length (mm) = 30 □, 28.1 △, 23 ○.

dependence on the anode length is observed. It is also important to observe that no radiation signals were detected for $V_p < 8$ kV (data without radiation are not shown in this graph).

Figure 5 shows the dependence of the x-ray signal on the pinch current intensity. It can be seen that the radiation emission is rather independent of this variable. This is a remarkable difference between the x-ray and the neutron emmision, since the latter is as a rule dependent on the pinch current [11, 12]. It can also be seen in the graph that the pinch current has some dependence on the anode length, likely due to its influence on the travelling time of the current sheet before forming a pinch, with respect to the current discharge period, which is substantially constant in this experiment because of the relatively large value (90 nH) of the fixed inductance in the discharge circuit.

Figure 6 shows the relationship between the pinch current and the voltage drop over the pinch. For $V_p > 10$ kV the current remains essentially independent of V_p. The solid symbols in the graph correspond to pinches that failed to produce radiation emission. It can be seen that there is a transition around $V_p \sim (8 \pm 2)$ kV separating the emitting–non emitting regions, marking a threshold for hard x-ray production.

In order to test whether there is a way to control the voltage drop over the pinch, in figure 7 V_p is plotted as a function of the charging voltage, V_o. It can be seen that there is a fuzzy correlation between both variables, but it should be stressed that the relation between V_p and V_o depends on the particular device and configuration. Actually, values of V_p up to three times larger than V_o are typical in a PF of some kiloJoules [7, 8, 16].

4. Discussion

The relationship between the voltage drop over the pinch and the hard x-ray intensity requires some discussion. At first sight, it could be thought that provided that there is an axial voltage drop of the order of tens of kilovolts along the pinch, a beam of electrons with this energy should exist, producing in turn x-rays of the corresponding energy upon impacting back on the

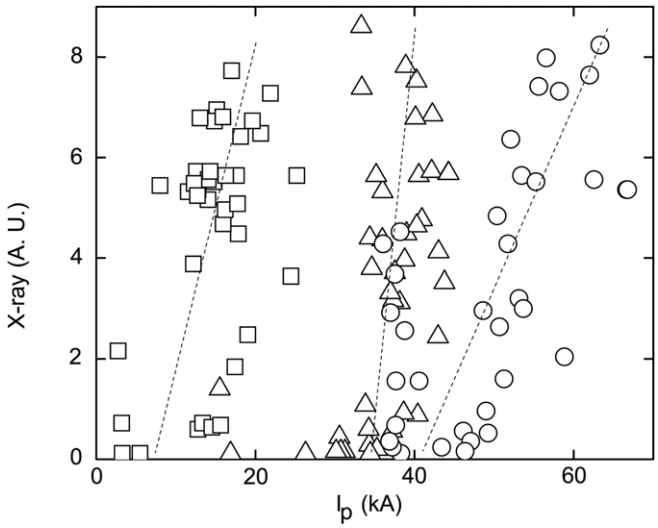

Figure 5. Hard x-ray intensity dependence on the pinch current intensity. Anode length (mm) = 30 □, 28.1 △, 23 ○.

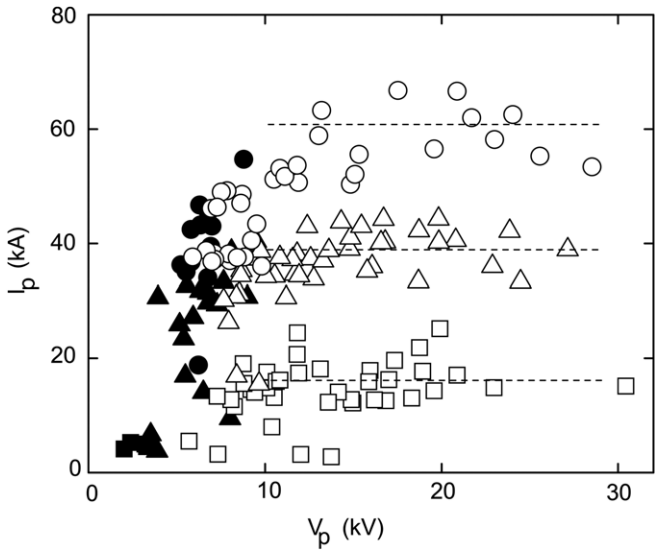

Figure 6. Dependence of the pinch current on the pinch voltage. Anode length (mm) = 30 □, 28.1 △, 23 ○. Empty and solid symbols represent pinches with and without radiation emission. It can be seen that the lowest pinch voltages fail to produce x-rays.

anode. However, the acceleration of electrons up to these energies does not necessarily follow, since the plasma is not collisionless; hence the electrons accelerated by the electric field are not free particles and therefore simply acquire a drift velocity. The generation of an electron beam is possible only in the cases in which the applied electric field V_p/d (d being the pinch length) exceeds the runaway Dreicer condition [13]. To calculate this condition an important

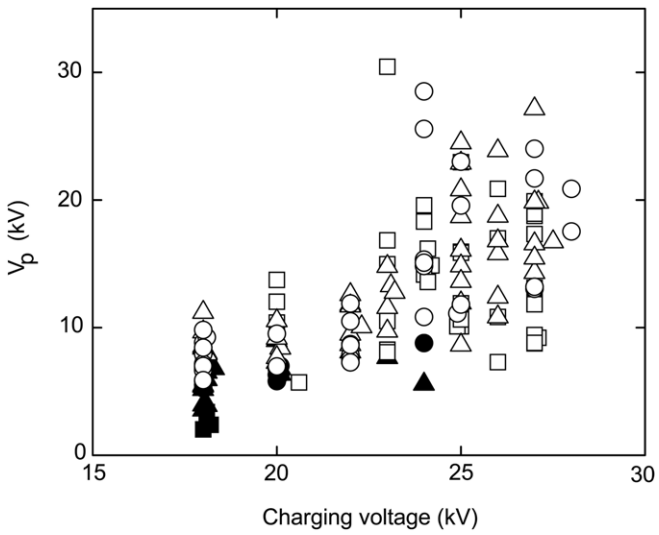

Figure 7. Dependence of the pinch voltage on the charging voltage. Anode length (mm) = 30 □, 28.1 △, 23 ○. Empty and solid symbols represent pinches with and without radiation emission.

parameter is the critical electric field E_c which is given by

$$E_c = n\left(\frac{m}{e}\right)4\pi\left(\frac{e^2}{4\pi\varepsilon_o m}\right)^2 \ln\Lambda\left(\frac{m}{2kT_e}\right),$$

where m, e and T_e are the electron mass, charge and temperature, respectively, n is the electron density, ε_o is the vacuum dielectric constant and $\ln\Lambda$ is the Coulomb logarithm. In practical units it can be written as

$$E_C\,[\mathrm{V\,m^{-1}}] \approx 3.9\times10^{-10}\frac{n\,[\mathrm{cm^{-3}}]}{kT\,[\mathrm{eV}]}.$$

A precise determination of the mentioned condition would require a knowledge of the electron density n and the temperature T_e, which are not available for the present experiment. However, some estimations can be done.

First, note that when the voltage between the electrodes and the current derivative peaks (and hence V_p also peaks) the plasma column reaches its maximum inductance rate of change (not its maximum inductance value). Therefore, this time is not that of 'maximum pinch compression', as frequently stated. Instead, at this time, the most likely plasma configuration is a relatively short central column with hollow CS portions still converging at both ends.

Second, the inductive nature of the voltage implies that the electric field is located in the regions of the plasma in which the current circulates, that is, the outer layers (due to the skin effect).

Electron densities in the converging CS and in the forming column have been measured in other devices being proportional to the charging pressure [14]. Based on this dependence, in our device $n \approx 10^{18}\,\mathrm{cm^{-3}}$ is a sensible assumption either for the CS and the external portions of a column.

Electron temperatures have been measured scarcely and with insufficient time resolution. However, its value can be estimated noting that the pinch has a shock nature, which primarily heats the ions, and that the electron–ion energy equilibration times are in the order of the pinch

evolution (i.e. the electron temperatures should be smaller than the ion temperatures most of the time). From the typical implosion velocity values, ion temperatures of $kT_e \sim 100$ eV can be expected. This yields a runaway electric-field threshold $E_c \sim 39\,\mathrm{kV\,cm^{-1}}$.

Assuming that the length of the forming pinch equals approximately the anode radius [6], the average electric field along the pinch in the present experiment is about $3V_p\ \mathrm{cm^{-1}}$. Taking into account the experimental threshold for hard x-ray production, (8 ± 2) kV (see figure 6), the corresponding runaway electric-field threshold results $(24 \pm 6)\,\mathrm{kV\,cm^{-1}}$. Considering that the high energy tail of the Maxwellian distribution can provide a sizable number of electrons in the runaway regime, the result is in good agreement with Dreicer theory.

5. Conclusions

The operation of a PF device of a few hundred Joules, without a cylindrical outer electrode and producing hard x-rays at 1.8 mbar D_2, was achieved. Neutrons were also produced, but below the detection level of the scintillator photomultiplier employed. Using three different anode lengths, the current amplitude at the pinch time was significantly varied, but this change in the pinch current did not influence the x-ray yield. Instead, the x-ray yield was strongly dependent on the total voltage drop in the forming pinch. A significant agreement between the minimum electric field in the pinch required for hard x-ray emission and that predicted by Dreicer for the electron runaway regime was found.

Acknowledgment

L Soto thanks the Bicentennial Program in Science and Technology grant ACT26, Center of Research and Applications in Plasma Physics and Pulse Power Technology (P^4-Project) Chile.

References

[1] Soto L, Moreno J, Silvester G, Zambra M, Pavez C, Altamirano L, Bruzzone H, Barbaglia M, Sidelnikov Y and Kies W 2004 Research on pinch plasma focus devices of hundred of kilojoules to tens of Joules *Braz. J. Phys.* **34** 1814–21

[2] Kasperczuk A, Paduch M, Pisarczyk T, Scholz M and Tomaszewski K 2002 Final stages of the plasma column evolution in the plasma-focus PF1000 device *IEEE Trans. Plasma Sci.* **30** 56–7

[3] Soto L, Pavez C, Moreno J, Barbaglia M and Clausse A 2008 Nanofocus ultra miniature pinch plasma focus device with submillimetric anode operating at 0.1 J *Plasma Sources Sci. Technol.* **18** 015007

[4] Soto L, Silva P, Moreno J, Zambra M, Kies G, Mayer R, Clausse A, Pavez C and Huerta L 2008 Demonstration of neutron production in a table-top pinch plasma focus device operating at only tens of Joules *J. Phys. D: Appl. Phys.* **41** 205215

[5] Verma R, Roshan M V, Malik F, Lee P, Lee S, Springham S V, Tan T L, Krishnan M and Rawat R S 2008 Compact sub-kilojoule range fast miniature plasma focus as portable neutron source *Plasma Sources Sci. Technol.* **17** 045020

[6] Lee S and Serban A 1996 Dimension and lifetime of the plasma focus pinch *IEEE Trans. Plasma Sci.* **24** 1101–5

[7] Di Lorenzo F, Raspa V, Knoblauch P, Lazarte A, Moreno C and Clausse A 2007 Hard x-ray source for flash radiography based on a 2.5 kJ plasma focus *J. Appl. Phys.* **102** 033304

[8] Moreno C, Raspa V, Sigaut L, Vieytes R and Clausse A 2006 Plasma-focus-based tabletop hard x-ray source for 50 ns resolution introspective imaging of metallic objects through metallic walls *Appl. Phys. Lett.* **89** 091502

[9] Neog N, Mohanty S and Borthakur T 2007 Time resolved studies on x-rays and charged particles emission from a low energy plasma focus device *Phys. Lett.* A **372** 2294–9

[10] Bruzzone H, Acuña H, Barbaglia M and Clausse A 2006 A simple plasma diagnostic based on processing the electrical signals from coaxial discharges *Plasma Phys. Control. Fusion* **48** 609–20

[11] Bruzzone H, Acuña H and Clausse A 2008 Neutron correlations with electrical measurements in a plasma focus device *Braz. J. Phys.* **38** 117–22

[12] Moreno C, Bruzzone H, Martínez J and Clausse A 2000 Conceptual engineering of plasma-focus thermonuclear pulsars *IEEE Trans. Plasma Sci.* **28** 1735–41
[13] Dreicer H 1959 Electron and ion runaway in a fully ionized gas *Phys. Rev.* **115** 238
Dreicer H 1960 Electron and ion runaway in a fully ionized gas *Phys. Rev.* **117** 329
[14] Bruzzone H and Fischfeld G 1989 On the structure of plasma focus imploding current sheaths *Phys. Lett.* A **134** 484
[15] Raspa V, Sigaut L, LloveraR, Cobelli P, Knoblauch P, Clausse A and Moreno C 2004 Plasma focus as a powerful hard x-ray source for ultrafast imaging of moving metallic objects *Braz. J. Phys.* **34** 1696–9
[16] Soto L 2005 New trends and futures perspectives on plasma focus research *Plasma Phys. Control. Fusion* **47** A361–81